

$$A_0A = l_1 = 220\text{mm}; AB = l_2 = 680\text{mm}; BC = l_3 = 240\text{mm};$$

$$CF = l'_3 = 620\text{mm}; DE = l_4 = 540\text{mm}; EF = l_5 = 440\text{mm}; FH = l'_5 = 120\text{mm}.$$

The maximum rotation angle of the crank shaft 1 is:

$$\angle A_i A_0 A_f = 260^\circ.$$

We draw the kinematics' scheme, on scale, for the angle $(x A_0 A_i) = \varphi_{1i}$, and the segment GCD is in vertical position, the points C and D are considered as fixed joints.

The initial position of the crank is $A_0 A_i$ when the elements 1 and 2 are in prolongation.

In the mechanism functioning we identify two phases [4]:

- The element 6 (with the points G, C and D) stays fixed until, through the crank shaft rotation, the point B reaches the vertical part of the element 6, between the points C and G;

- All the kinematics elements of the mechanism are joining rigid, also continuing the crank shaft rotation until the end position $A_0 A_f$, the mechanism becomes as a rigid body, which rotates upon the fixed joint A_0 . The trajectories of all mobile joints are circles with the centre in A_0 joint.

2. THE KINEMATICAL ANALYSIS OF THE MANIPULATOR MECHANISM

The position of the point A^* (implicitly the angle $\angle A_i A_0 A^*$), for which the angle $\varphi_3 = 180^\circ$, is determined resolving the nonlinear system of scalar equations:

$$x^2 + y^2 = l_1^2; \tag{1}$$

$$(x - x_c + l_3)^2 + (y - e)^2 = l_2^2. \tag{2}$$

where: $l_1 = 220\text{mm}; l_2 = 680\text{mm}; l_3 = 240\text{mm}; x_c = CG = 680\text{mm}; e = 100\text{mm}.$

Resolving the system formed by the equations (1) and (2) we obtain the point A^* coordinates, for which the angle $\varphi_3 = 180^\circ$. This are, $x = -210,60\text{ mm}, y = -63,61\text{ mm}.$

We consider the angular velocity of the crank shaft as being 1 rad/s. With that motion law for the motor element, we represent in figure 2, the time variation law of the angular position, in degrees, of the crank shaft.

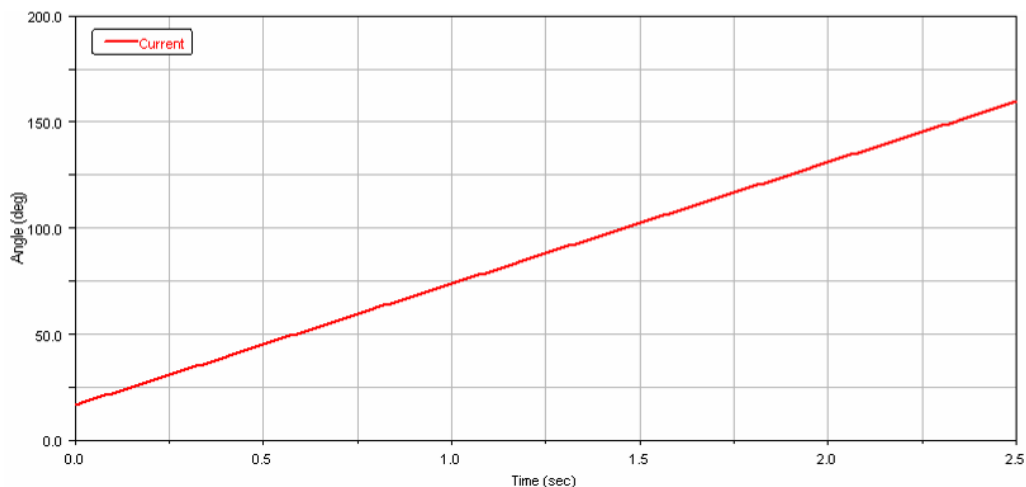


Fig. 2. Law of variation of the crank rotation angle, in degrees

The analytical calculus of the angles φ_2 and φ_3 , is made by solving the following scalar equations systems (fig. 1):

$$l_2 \cos \varphi_2 - l_3 \cos \varphi_3 = l_6 - l_1 \cos \varphi_1; \tag{3}$$

$$l_2 \sin \varphi_2 - l_3 \sin \varphi_3 = e - l_1 \sin \varphi_1. \quad (4)$$

where: $l_6=CG=680\text{mm}$; $e=100\text{mm}$.

In figures 3 and 4 we have represented the laws of variations in time for the angles φ_2 and φ_3 . We observe that the angle φ_2 starts from 16,47 degree and the angle φ_3 starts from 40 degree.

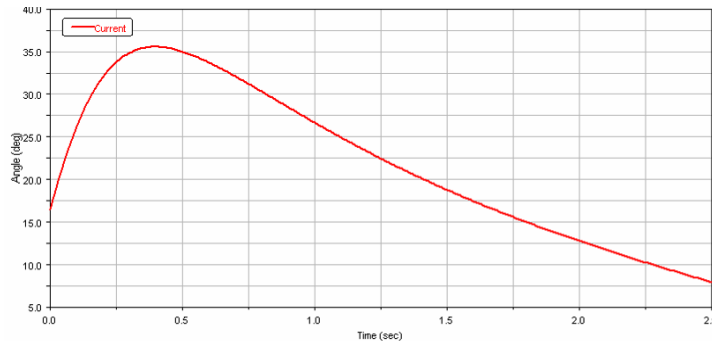


Fig. 3. Time variation law of the angle φ_2

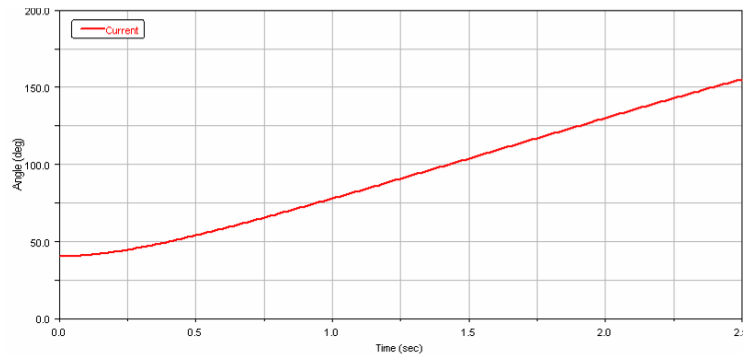


Fig. 4. Time variation law of the angle φ_3

The analytical calculus of the angles φ_4 and φ_5 (upon the angle φ_3) is made by solving the following scalar equations system (fig. 1):

$$l_4 \cos \varphi_4 + l_5 \cos \varphi_5 = l'_6 + l'_3 \cos \varphi_3; \quad (5)$$

$$l_4 \sin \varphi_4 + l_5 \sin \varphi_5 = l'_3 \sin \varphi_3. \quad (6)$$

where: $l'_6 = 380\text{mm}$; $l'_3 = 620\text{mm}$; $l_4 = EF = 440\text{mm}$; $l_5 = DE = 540\text{mm}$.

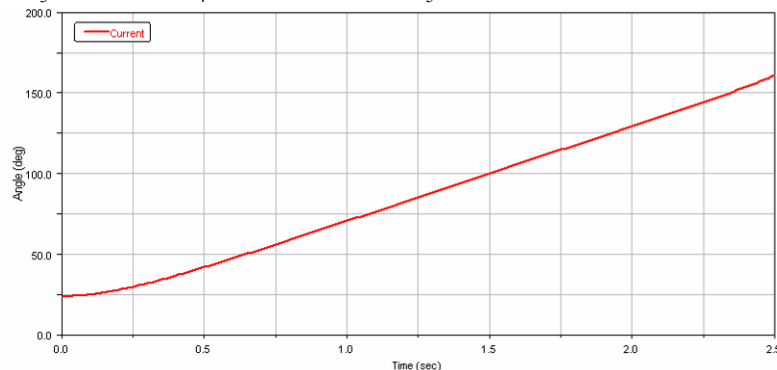


Fig. 5. Time variation law of the angle φ_4

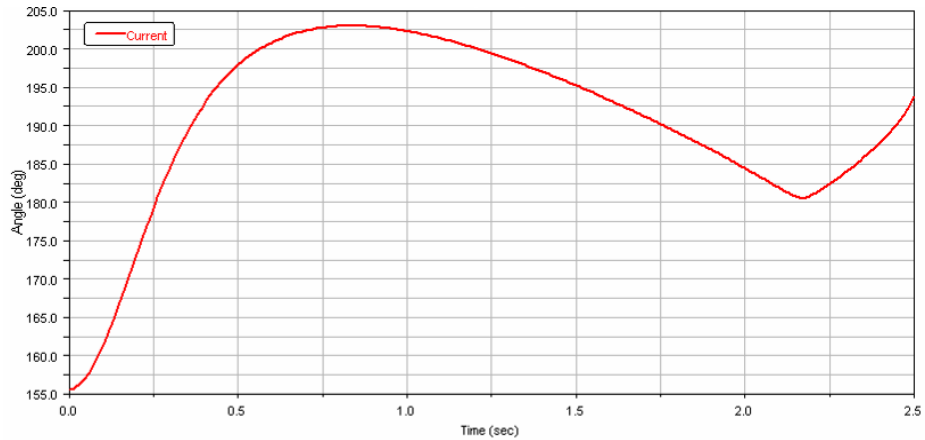


Fig. 6. Time variation law of the angle φ_5

We establish the Cartesian coordinates of the point H (figure 1), which depends by the point F coordinates and by the angle φ_5 , calculated previously [1]:

$$x_H = l_6 + l'_3 \cdot \cos \varphi_3 + l'_5 \cdot \cos \varphi_5; \tag{7}$$

$$y_H = e + l'_3 \cdot \sin \varphi_3 + l'_5 \cdot \sin \varphi_5. \tag{8}$$

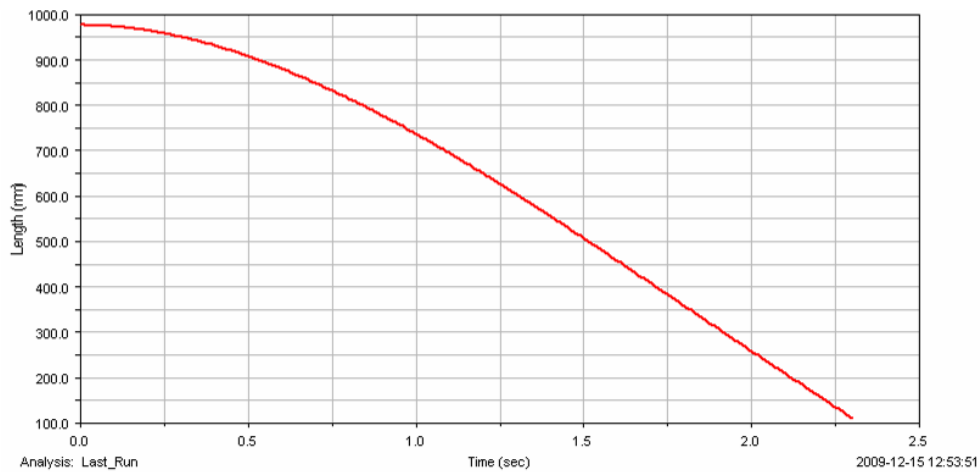


Fig. 7. Time variation of the coordinate x_H

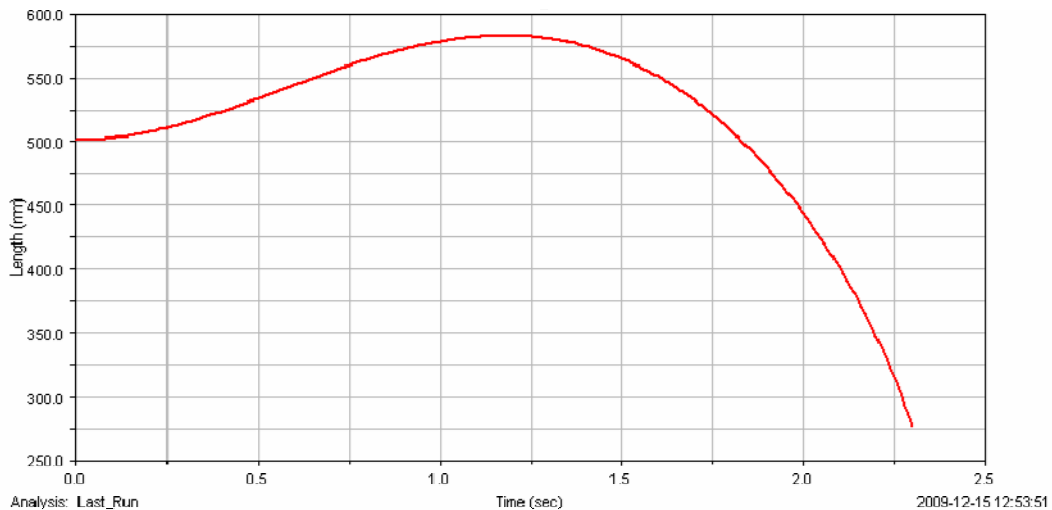


Fig. 8. Time variation of the coordinate y_H

We observe, from figure 7 and 8, that the coordinate x_H decrease from approximately 1000 mm to 100 mm, and the coordinate y_H varies from 580 mm to 275 mm. The curve described by the point H, is represented in figure 9. We also have represented, in figures 10 and 11, the components of the linear speed and acceleration of the point H.

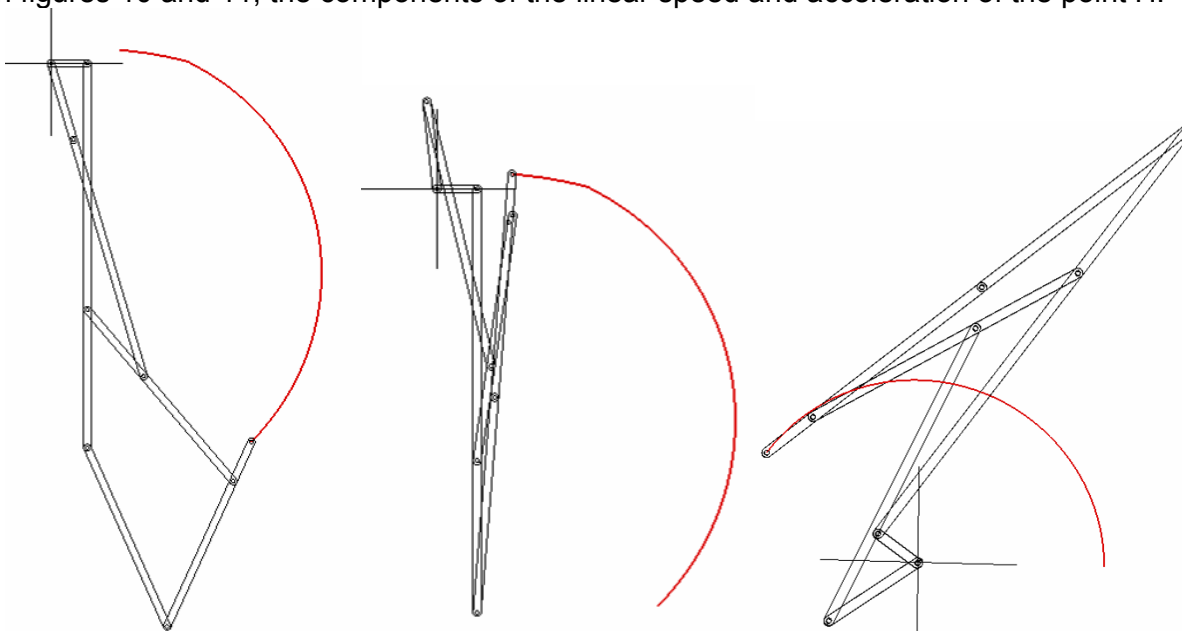


Fig. 9. The trajectory described by the point H

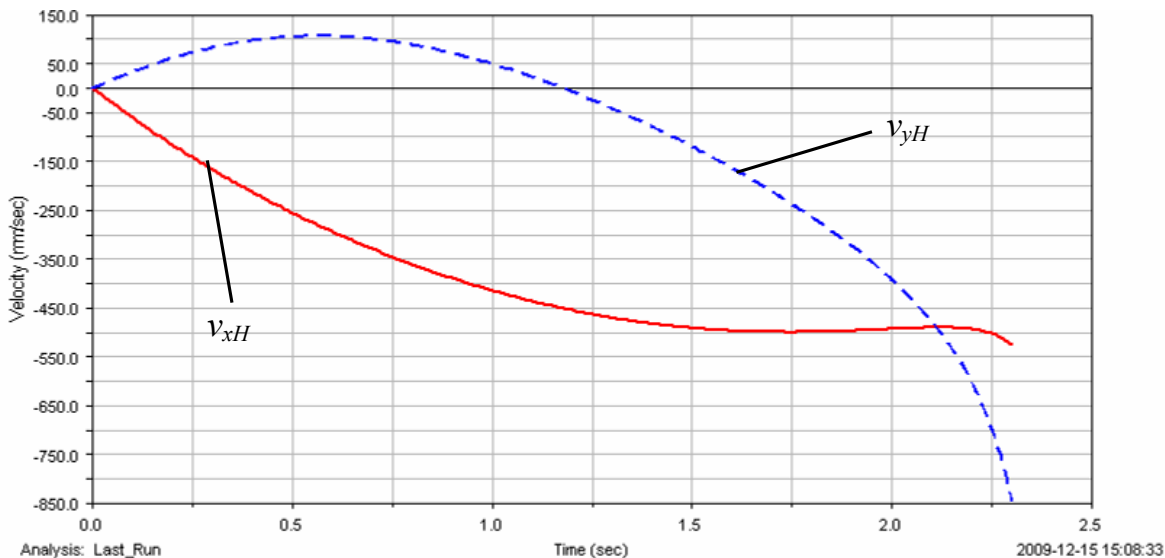


Fig. 10. The linear velocity components of the point H, in mm/s

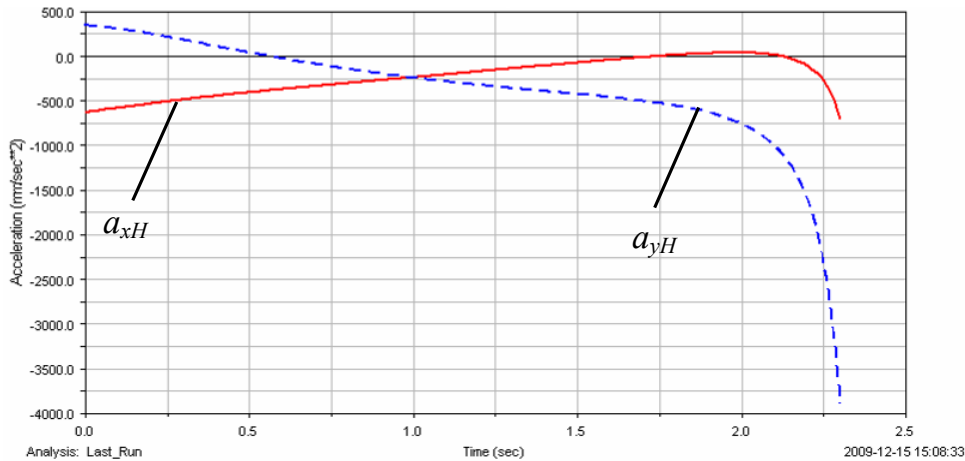


Fig. 11. The linear acceleration components of the point H, in mm/s²

The motor torque variation, $M_{m1} = M(\varphi_1)$, at the crank shaft 1, with a technological resistant force $F_r = G_H = 1000$ N (figure 1), is represented in figure 12.

The motor torque is obtained from the formula [1, 5]:

$$M_{m1} = F_r \frac{v_{xH}}{\omega_1} \tag{9}$$

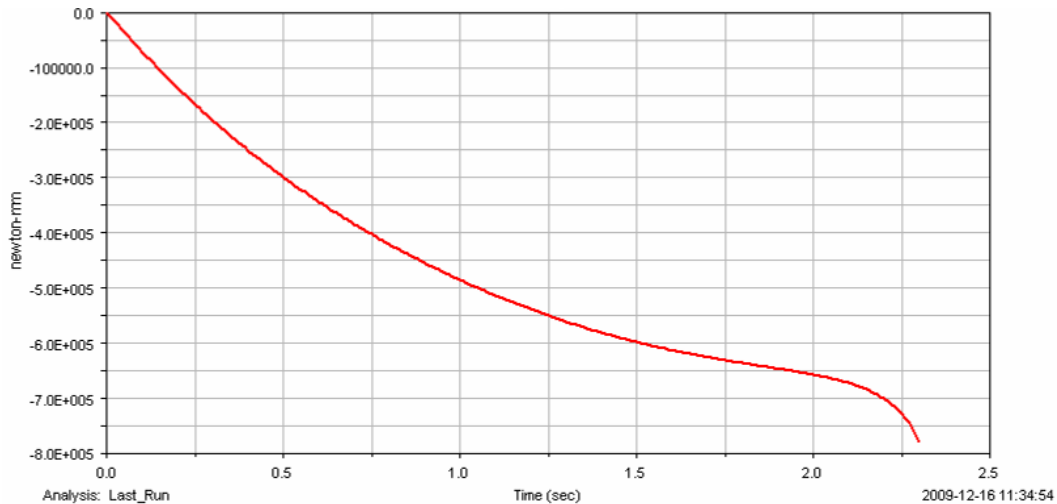


Fig. 12. The motor torque variation law, in Nmm

REFERENCES

[1]. Antonescu, P., Mechanism and Machine Science, Ed. Printech Bucharest, 2005.
 [2]. Antonescu, O., Coltofeanu, R., Antonescu, P., Geometria manipuloarelor pentru descărcarea recipientelor cu reziduuri gunoiere, Revista Mecanisme și Manipuloare, Vol. 5, Nr. 2, p. 25-30, 2006.
 [3]. Antonescu, O., Antonescu, P., Mihalache, D., Geometry of lifting manipulators for green environment, Rev. Robotica și Management, Vol., 11, Nr. 1, p. 35-40, 2006.
 [4]. Antonescu, O., Mihalache, D., Antonescu, P., Lifting manipulators for a green environment, Twelfth world congress in Mechanism and Machine Science, Besancon – Franța, Poceedings vol. 3, p. 205-212, 2007.
 [5]. Dumitru, N., Nanu, Gh., Vintilă D., Mecanisme și transmisii mecanice - Tehnici de modelare clasice și moderne, Editura Didactică și Pedagogică, București, 2008.